Available online at www.sciencedirect.com
SCIENCE DIRECT
Biochemical Pharmacology 70 (2005) 1066–1078
Biochemical Pharmacology
www.elsevier.com/locate/biochempharm

Inhibitory effects of rosmarinic acid on adriamycin-induced apoptosis in H9c2 cardiac muscle cells by inhibiting reactive oxygen species and the activations of c-Jun N-terminal kinase and extracellular signal-regulated kinase

Do-Sung Kim [a], Hyung-Ryong Kim [b], Eun-Rhan Woo [c], Seong-Tshool Hong [d], Han-Jung Chae [a,**,1], Soo-Wan Chae [a,*,1]

[a] *Department of Pharmacology and Institute of Cardiovascular Research, School of Medicine, Chonbuk National University, Jeonju, Chonbuk 560-180, South Korea*
[b] *Department of Dental Pharmacology and Nano-Science & Technology Research Institute, School of Dentistry, Iksan, Chonbuk, South Korea*
[c] *Chosun University, College of Pharmacy & Research Center for Proteineous Materials, Gwangju, South Korea*
[d] *Department of Microbiology, School of Medicine, Chonbuk University, Jeonju, South Korea*

Received 17 December 2004; accepted 28 June 2005

Abstract

Rosmarinic acid (RA) is a naturally occurring polyphenolic and is found in several herbs in the *Lamiaceae* family, such as, *Perilla frutescens*. ADR is a potent anti-tumor drug, but is unfortunately potently cardiotoxic. This study was undertaken to investigate the inhibitory effect of RA on ADR-induced apoptosis in H9c2 cardiac muscle cells at a mechanistic level. In vitro, ADR significantly decreased the viabilities of H9c2 cells, and this was accompanied by apoptotic features, such as a change in nuclear morphology and caspase protease activation. RA was found to markedly inhibit these apoptotic characteristics by reducing intracellular ROS generation and by recovering the mitochondria membrane potential ($\Delta\psi$). In addition, RA reversed the downregulations of GSH, SOD and Bcl-2 by ADR. In the present study, ADR was found to activate c-Jun N-terminal kinase (JNK) and extracellular signal-regulated kinase (ERK), transcriptional factor-activator-protein (AP)-1. We found that c-fos, Jun-B, Jun-D and p-c-Jun were super shifted by ADR, indicating that these proteins have an important role in the ADR-induced AP-1 activation. The inhibitions of JNK and ERK using appropriate inhibitors or dominant negative cell lines reduced ADR-induced apoptosis in H9c2 cardiac muscle cells. Taken together, these results suggest that RA can inhibit ADR-induced apoptosis in H9C2 cardiac muscle cells by inhibiting ROS generation and JNK and ERK activation. Thus, we propose that RA should be viewed as a potential chemotherapeutic that inhibits cardiotoxicity in ADR-exposed patients.

Keywords: Rosmarinic acid; ROS; Adriamycin; JNK; ERK; AP-1; Apoptosis

1. Introduction

ADR is a quinone-containing anti-cancer drug that is widely used to treat different types of human neoplastic diseases and a wide range of solid tumors, including those of the breast, lung and thyroid [1–3]. However, the clinical usefulness of this drug is severely restricted because of the development of severe cardiomyopathy or congestive heart failure years after ADR therapy [4,5]. Significant efforts have been directed toward developing an adjunctive therapy that reduces ADR-induced cardiotoxicity and enhances its therapeutic efficacy. The putative mechanism of ADR-induced

Abbreviations: ADR, ADR; AP-1, activator protein-1; BCA, bicinchoninic acid; CAT, catalase; $DiOC_6(3)$, 3,3′-diexyloxocarbocyanine iodide; DMEM, Dulbecco's modified Eagle's medium; DMSO, dimethyl sulfoxide; DN, dominant negative; EMSA, electrophoretic mobility shift assay; ERK, extracellular signal-regulated kinase; FBS, fetal bovine serum; GSH, glutathione; JNK, c-Jun N-terminal Kinase; MAN, mannitol; MAPK, mitogen-activated protein kinase; NAC, *N*-acetyl-cysteine; RA, rosmarinic acid; ROS, reactive oxygen species; SOD, superoxide dismutase

* Corresponding author. Tel.: +82 63 270 3089; fax: +82 63 275 2855.
** Corresponding author. Tel.: +82 63 270 3092; fax: +82 63 275 2855.
E-mail address: soowan@chonbuk.ac.kr (S.-W. Chae).
[1] Authors contributed equally to this work.

0006-2952/$ – see front matter © 2005 Elsevier Inc. All rights reserved.
doi:10.1016/j.bcp.2005.06.026

cardiotoxicity involves its redox activation to a semi-quinone intermediate and the formation of ROS, the latter of which induces myocyte apoptosis [6]. The involvement of ROS is evidence by the finding that ROS scavengers can inhibit ADR-induced cardiomyocyte apoptosis [7]. Pharmacological and clinical attempts to reduce ADR cardiotoxicity have only been partially successful, potential species identified include, ROS scavengers such as superoxide dismutase (SOD), catalase and mannitol [8,9].

Rosmarinic acid (RA), a natural phenolic is found in many *Lamiaceae* herbs, such as *Perilla frutescens*, sage, basil and mint. RA has been reported to inhibit complement-dependent inflammatory processes [10] and may have therapeutic potential [11]. Moreover, the medicinal value of RA has been well recognized, especially in regard to its anti-oxidant and anti-inflammatory activities [12,13]. However, the mechanism underlying these RA-induced effects on the cardiovascular system is unknown. Therefore, in this study we examined the effects of RA on ADR-damaged cardiac muscle cells in the hope of elucidating its mode of action (Fig. 1).

2. Materials and methods

2.1. Reagents

RA was isolated from *L. lucidus* (Labiatae) [14]. Dulbecco's Modified Eagle medium (DMEM), fetal bovine serum (FBS), trypsin and other tissue culture reagents were purchased from Life Technologies, Inc. (Gaithersburg, MD). Bicinchoninic acid (BCA) protein assay reagents were from Pierce; ADR was from Sigma; the annexin V-FITC apoptosis detection kits (6993KK) were from PharMingen (San Diego, CA) and 3,3′-diexyloxocarbo-cyanine iodide ($DiOC_6(3)$) was from Molecular Probes (Eugene, Oregon). All other chemicals were purchased from either Sigma or Aldrich (St. Louis, MO). All reagents were of at least analytical grade, and plastic ware was purchased from Falcon Inc. (Franklin Lakes, NJ).

2.2. Cell culture and viability

The H9c2 rat cardiomyoblast cell line (ATCC, CRL-1446) was maintained in DMEM containing 10% (v/v) heat-inactivated FBS, penicillin G (100 U/mL), streptomycin (100 mg/mL) and L-glutamine (2 mM). RA was dissolved in DMSO and added to wells at a final concentration of 20 μg/mL; the DMSO content never exceeded 0.1%. Cells were incubated for 30 min before adding ADR. H9c2 cells were then assessed with microscope for dead cells by Trypan blue exclusion. Cell viability was calculated by dividing the non-stained (viable) cell count by the total cell count.

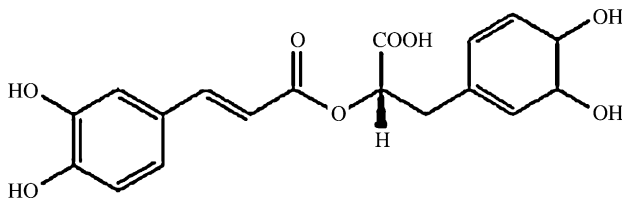

Fig. 1. Chemical structure of rosmarinic acid isolated from digitalis purpurea.

2.3. Plasmids and transfections

Empty pcDNA3-vector (Invitrogen), or pcDNA3 containing dominant-negative ERK (DN) (Invitrogen) or dominant-negative (DN) JNK (Invitrogen) were transfected into H9c2 cells (grown in six-well plates) using LipofectAMINE Plus, according to the manufacturer's instructions (Life Technologies, Inc.). Transfections were performed without serum for 3 h. Cells were selected for resistance to neomycin (1.0 μg/mL) 2 days after transfection. Pools of transfectants and individual clones (between 5 and 33) were isolated and selected for further analysis.

2.4. Fluorescent staining of nuclei

H9c2 nuclei were stained with chromatin dye (Hoechst 33258). Briefly, cells were fixed with 3.7% paraformaldehyde for 10 min at room temperature, washed twice with PBS, and incubated with 10 μM Hoechst 33258 in PBS at room temperature for 30 min. After three washes, cells were observed under a fluorescence microscope (MPS 60, Leica). For c-Jun or phospho-c-Jun staining, the cells were fixed with acetone/methanol (50:50) for 3 min at −20 °C. Following fixation, they were blocked with 10% fetal bovine serum in PBS for 1 h, incubated for 24 h at 4 °C with antibody against c-Jun or phosphor-c-Jun at 1:100 dilution in PBS containing 3% bovine serum albumin, washed with PBS and incubated for an additional hour at room temperature with Cy2-conjugated anti-rabbit IgG at a dilution of 1:800 in PBS containing 3% bovine serum albumin. The cells were then viewed under a fluorescence microscope (Axioplan 2, Carl Zeiss).

2.5. Preparation of cell extracts

Cells were harvested by centrifugation, washed with PBS, and re-suspended in 0.1 mL of lysis buffer containing 1% Triton X-100, 10 mM Tris, pH 7.6, 50 mM NaCl, 0.1% bovine serum albumin (BSA), 1 mM phenylmethyl sulfonyl fluoride (PMSF), 1% aprotinin, 5 mM EDTA, 50 mM NaF, 0.1% 2-mercaptoethanol, 5 mM phenylarsine oxide and 100 mM sodium orthovanadate. After lysis on ice for 30 min, cell lysates were cleared by centrifugation at 14,000 × *g* at 4 °C for 20 min.

2.6. Western blotting analysis

After treating cells with ADR in the presence or absence of RA, they were lysed, and identical amounts of lysates

(50 μg of protein) was added to equal volumes of 3× sample buffer, boiled at 98 °C for 5 min, and then separated by 10% SDS-polyacrylamide gel electrophoresis (SDS-PAGE). After electrophoresis, proteins were transferred to PVDF membranes using a semi-dry electrophoretic transfer system (Alert Inc.). Membranes were incubated in 5% dried skim milk at room temperature for 1 h and incubated with Bcl-2, Bax, phospho-JNK, phospho-ERK, phospho-p38, JNK, ERK, p38, phospho-ATF-2, phospho-c-Jun, JNK, ERK, p38, c-Jun, Jun-B, Jun-D, or actin primary antibodies at room temperature for 2 h. Antibody recognition was detected using the respective secondary antibody, either anti-mouse or anti-rabbit IgG_1 linked to horseradish peroxidase at room temperature for 60 min. Expression levels were normalized versus β-actin. Immunoreactive bands were visualized using an enhanced chemiluminescence (ECL) kit (Amersham) and exposed to LAS 3000 (Fuji Film).

2.7. Determination of caspase-3 activity

H9c2 cells (3×10^6) were washed with PBS and incubated for 30 min on ice with 100 mL of lysis buffer (10 mM Tris–HCl, 10 mM NaH_2PO_4/$NaHPO_4$, pH 7.5, 130 mM NaCl, 1% Triton1 X-100 and 10 mM sodium pyrophosphate). Cell lysates were spun down, supernatants were collected, and protein concentrations determined using the BCA method. For each reaction, 30 μg of protein was added to 1 mL of freshly prepared protease assay buffer (20 mM HEPES pH 7.5, 10% glycerol, 2 mM dithiothreitol) containing 20 mM of AC-DEVD-AMC (Sigma–Aldrich). Reaction mixtures without cellular

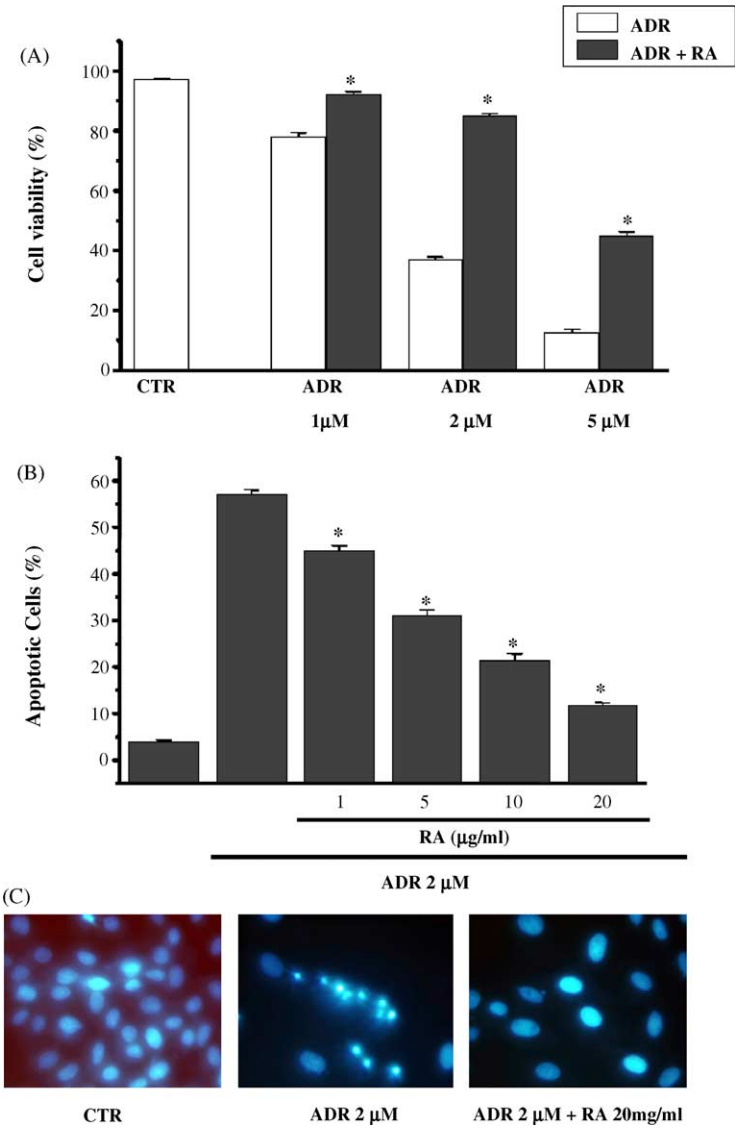

Fig. 2. The inhibitory effect of rosmarinic acid on H9c2 cell death caused by ADR. Cell death was assessed by Trypan Blue assay and morphology. (A) Cells were pretreated with rosmarinic acid (20 μg/mL) for 30 min and then treated with the indicated concentrations (1, 2, 4 μM) of ADR for 30 h. (B) Cells were pretreated with rosmarinic acid (1, 5, 10, 20 μg/mL) for 30 min and then with ADR 2 μM for 30 h. (C) Cells were pretreated with rosmarinic acid (20 μg/mL) for 30 min, and then with ADR 2 μM for 30 h. The cells were stained with Hoechst 33258 and observed under a fluorescence microscope. Data represent means ± S.E. ($n = 5$). $^*P < 0.01$; significantly different from ADR-treated H9c2 cells.

extracts were used as negative controls. Reaction mixtures were incubated for 1 h at 37 °C and the aminomethylcoumarin liberated from AC-DEVD-AMC was determined by spectrofluorometry (Hitachi F-2500) at 380 nm excitation and 400–550 nm emission. Readings were corrected for background fluorescence.

2.8. Cytofluorometric assessment of mitochondrial membrane potential

A stock solution of $DiOC_6$ (4 mmol/L) was prepared in ethanol and stored in small lots at −20 °C; working solution (dilution 1:2000 for $DiOC_6(3)$) was made up in experimental medium (DMEM) immediately before use. A total of 5×10^5 H9c2 cells were incubated in DMEM containing 100 nM $DiOC_6(3)$ at 37 °C, and analyzed using a PAS cytofluorometer (Partec) equipped with Partec software. Forward and side scatters were gated for the major population of normally sized cells and a minimum of 10,000 cells was analyzed. The fluorescent probe $DiOC_6$ was excited using a 488 nm argon laser, and emissions were collected through an FL1 detector fitted with a 525 ± 5 nm band pass filter.

2.9. DCFDA assay

Cells were incubated with 2 μM ADR and 500 μM H_2O_2 in the absence or presence for 30 min or 16 h and then treated with 100 μM 2′,7′-dichlorofluorescin diacetate (DCF-DA; Molecular Probes) at 37 °C for an additional 30 min. After chilling on ice, cells were washed with cold PBS, removed by scraping, and resuspended at 1×10^6 cells/mL in PBS containing 10 mM EDTA. The fluorescence intensities of 2′,7′-dichlorofluorescein formed by reaction between DCF-DA and the intracellular ROS of >10,000 viable cells in each sample were analyzed by PAS Vantage flow cytometry (Partec) 488 nm excitation and 525 nm emission, respectively. Data were collected and analyzed using Becton Dickinson Partec software. Experiments were repeated at least three times with similar results. Data are expressed as histograms representative of three independent experiments.

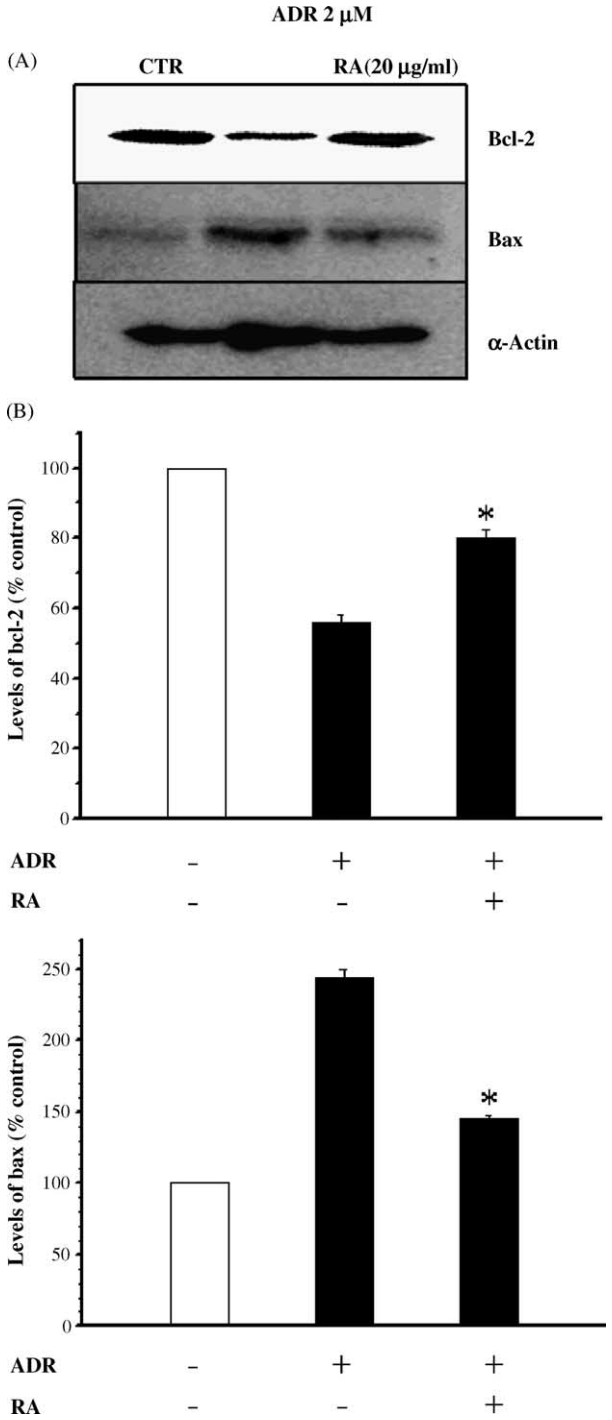

Fig. 3. The preventive effect of RA on ADR-modulated Bcl-2 expression. (A) H9c2 cells were pretreated with 20 mg/ml RA for 30 min and then treated with 2 mM ADR for 30 h. Bcl-2 family protein expressional changes were analyzed by Western blotting with anti-Bcl-2, anti-Bax and anti-a-actin (loading control) antibodies. Immunoreactive bands were visualized by LAS-3000 (FUJI FILM). (B) The quantitative densitometric scanning results were shown. The data shown represent means ± S.E. ($n = 3$). $^*P < 0.01$; significantly different from ADR only treated H9c2 cells.

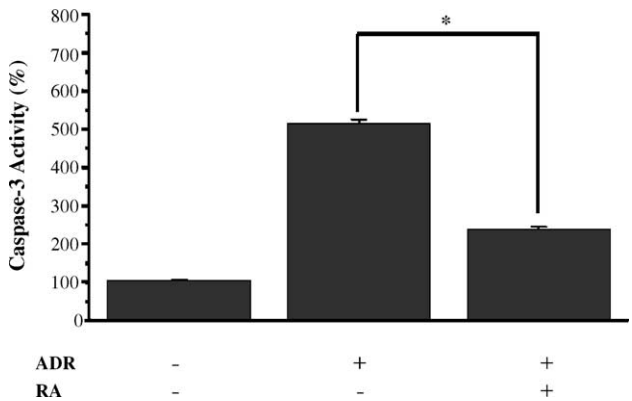

Fig. 4. The inhibitory effect of rosmarinic acid on caspase-3 activity induced by ADR. Cells were pretreated with 20 μg/mL rosmarinic acid for 30 min and then treated with 2 μM ADR for 6 h. Caspase-3 activity in the cytosolic fraction was monitored by measuring the absorbance of the cleaved fluorogenic substrate, AMC-DEVD. Data represent means ± S.E. ($n = 3$). $^*P < 0.001$; significantly different from ADR only treated H9c2 cells.

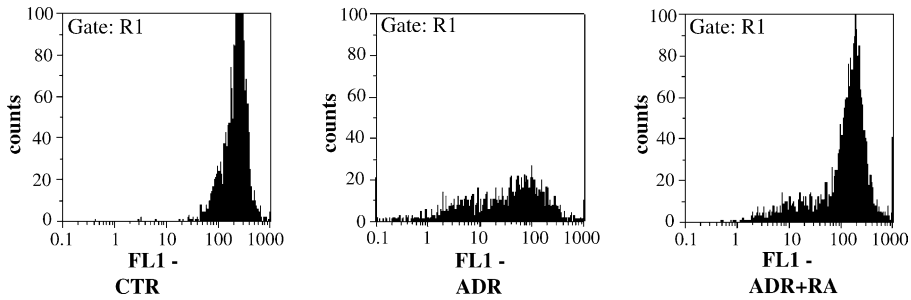

Fig. 5. The reversal of ADR-induced mitochondrial membrane potential ($\Delta\Psi_m$) collapse by rosmarinic acid. Cells were treated with 2 μM ADR for 24 h in the absence or presence of rosmarinic acid (20 μg/mL), and then incubated with $DIOC_6$ (100 nM). Fluorescence intensities of lots of 10,000 cells were determines by flow cytometry (Partec PAS). Control cells, Cells treated with ADR, or cells treated with ADR followed by RA.

2.10. Measurement of total glutathione in ADR-treated H9c2 cells

After treating H9c2 cells with 2 μM ADR in the presence or absence of 20 μg/mL RA, 3×10^6 cells were washed with PBS and incubated for 30 min on ice, centrifuged, lysed with 0.5 mL of freshly prepared 1% (w/v) sulfosalicylic and placed on ice for 15 min. They were then centrifuged for 5 min at 10,000 × *g* and total glutathione in supernatant was measured as previously described [15] with minor modifications. Briefly, 100 mL of 0.1N HCl was mixed with DTNB-containing buffer (110 mM Na_2HPO_4, 40 mM NaH_2PO_4, 0.04% (w/v) bovine serum albumin, 15 mM EDTA and 0.3 mM DTNB), and to this mixture were added 100 mL of sample and 200 mL reagent mix (50 mM HCl–imidazole (pH 7.2), 0.02% bovine serum albumin, 2 mM NADPH and 1 unit/mL of Type IV yeast glutathione reductase). A calibration curve was prepared using GSH (0.3–50 mM) freshly prepared in 1% sulfosalicylic acid. Optical density at 412 nm was read for 10 min at room temperature. Glutathione concentrations per 10^{10} cells were calculated.

2.11. Electrophoretic mobility shift assay

The probe used for electrophoretic mobility shift assays (EMSA) was a 22-bp double-stranded construct with the AP-1 consensus binding sequence (5′-CGCTTGATGACTCAGCCGGAA-3′). Probe end labeling was achieved using T_4 kinase and (γ-^{32}P) ATP. EMSAs were performed using nuclear extracts (10 μg) from RA-treated or non-preteated cells with or without ADR treatment. Specific competition was induced by adding 200 ng of unlabeled double-stranded 22-bp probe. Protein–DNA complexes were analyzed by electrophoresis on a 4% non-denaturing polyacrylamide gel. Gels were then vacuum-dried and autoradiographed.

2.12. Statistical analysis

Statistical differences were evaluated in dose–response experiments by analysis of variance (ANOVA) and in hemodynamic variables over time between the control and treatment groups were assessed by the two-tailed Student's *t*-test. Other tests used are indicated as appropriate and experiment numbers are included in figure legends.

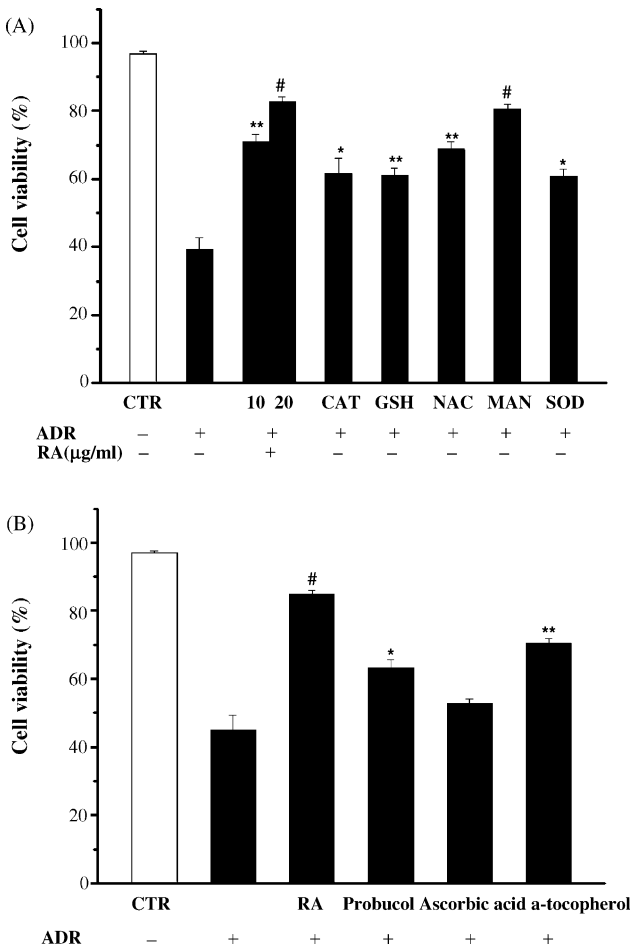

Fig. 6. The inhibitory effects of rosmarinic acid, anti-oxidant molecules, and anti-oxidants on H9c2 cell death induced by ADR. Cell death was assessed by Trypan Blue assay and morphology. (A) Cells pretreated with/without rosmarinic acid (10, 20 μg/mL), catalase (4×10^4 U/L), GSH (15×10^{-3} mol/L), NAC (10^{-4} mol/L), MAN (2×10^{-2} mol/L) or SOD (1.2×10^5 U/L) were treated with 2 μM ADR (B) Cells pretreated with/without rosmarinic acid (20 μg/mL), probucol (10^{-4} mol/L), ascorbic acid (5×10^{-5} mol/L), or alpha-tocopherol (10^{-4} mol/L) were treated with 2 μM ADR. The data shown represent means ± S.E. ($n = 5$). $^{*}P < 0.05$, $^{**}P < 0.01$, $^{\#}P < 0.001$; significantly different from ADR only treated H9c2 cells.

3. Results

3.1. Rosmarinic acid-induced cell resistance to ADR-induced cytotoxicity and apoptosis in H9c2 cells

In order to determine if RA modifies ADR-induced responses in H9c2 cells, cells were exposed to RA (20 μg/mL) and then stimulated with ADR (1, 2 or 4 μM). Fig. 2A shows the effect of treatment of RA on the cytotoxicity exerted by ADR in this cell line over a period of 30 h. At concentrations >0.1 mg/mL RA was found to inhibit against ADR-induced cell death (Fig. 2B). Maximum RA inhibition of ADR-induced toxicity (at an ADR concentration 2 μM) was observed at 10 or 20 μg/mL by Hoechst staining. The percentages of apoptotic cells observed in the presence or absence of RA (20 μg/mL) are shown in Fig. 2C, at this concentrations RA inhibited ADR-induced apoptosis from 55 ± 3.1 to $8 \pm 2.9\%$ ($n = 5$).

3.2. RA modulates Bcl-2 protein expression in ADR-treated H9c2 cells

Bcl-2 proteins promote cell survival and suppress the apoptotic cell death [16]. Therefore, we examined whether the expressions of mitochondrial membrane-associated Bcl-2 proteins are modulated by ADR. Accordingly, H9ce cells were preteated with 20 μg/mL RA for 30 min and then treated with 2 μM ADR for 30 h (Fig. 3). ADR treatment markedly reduced the expression of anti-apoptotic Bcl-2, and increased the expression of pro-apoptotic Bax. Consistent with its inhibitory effects, RA prevented this downregulation of Bcl-2 and markedly suppressed increased Bax expression (Fig. 3). β-actin was

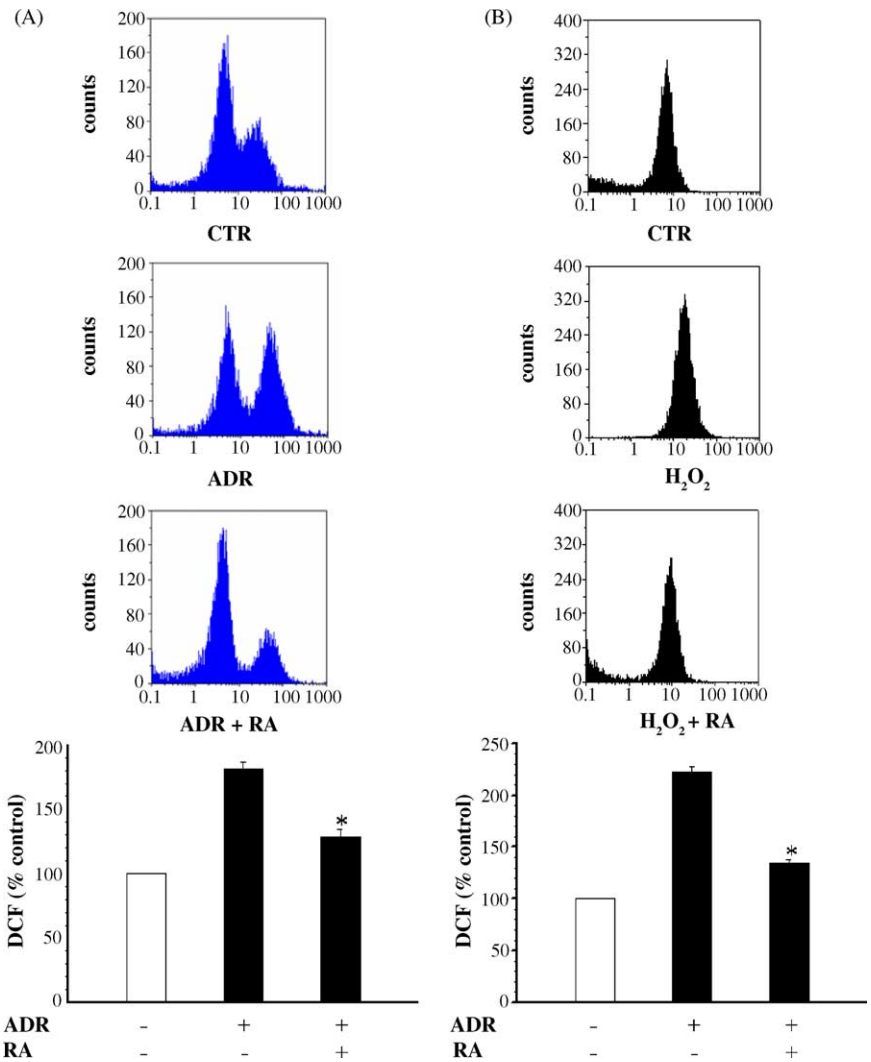

Fig. 7. The inhibitory effects of rosmarinic acid on intracellular ROS induced ADR or on H_2O_2. (A) Cells pretreated with/without rosmarinic acid (20 μg/mL) for 30 min and then with 2 μM ADR. (B) Cells were pretreated with/without rosmarinic acid (20 μg/mL) for 30 min and then with 500 μM H_2O_2. In both cases, cells were incubated with the dye 2′,7′-dichlorofluorescin diacetate (100 μM) and the fluorescence intensities of lots of 10,000 cells were analyzed by flow cytometry (Partec PAS). Data represent means ± S.E. ($n = 3$). $^*P < 0.01$; significantly different from ADR only treated H9c2 cells.

used as a loading control to confirm the natures of the Bcl-2 and Bax changes.

3.3. RA inhibit ADR-induced caspase-3 activation in H9c2 cells

Caspase cascade activation is critical for apoptotic initiation in many biological systems [17]. To determine whether caspase-3 participates in ADR cytotoxicity, we monitored its catalytic activity. It was found that its catalytic activity significantly increased in a time-dependent manner up to five-fold after ADR treatment, and that this peaked at 6 h (data not shown). However, RA completely abolished this activation (Fig. 4).

3.4. RA prevents ADR-induced mitochondria membrane potential ($\Delta\Psi_m$) collapse in H9c2 cardiac muscle cells

To elucidate the effect of RA on mitochondrial membrane potential, cells were pretreated with 20 μg/mL RA for 30 min and then treated with 2 μM ADR for 24 h. Mitochondria membrane potential was then monitored by flow cytometry using $DiOC_6$. This analysis showed that ADR reduced mitochondrial membrane potential, and that pre-treatment with RA blocked this reduction (Fig. 5)

3.5. RA regulates intracellular ROS

The chemoprotective effects of caffeic (CA), chlorogenic (CHA) and rosmarinic (RA) acids against ADR toxicity have been previously examined in neonatal rat cardiomyocytes, and RA was found to have the greatest effect, and incidentally, the strongest anti-oxidant activity [12,13]. To compare the anti-oxidant activity of RA with that of known anti-oxidants, we examined the effects of RA, catalase (CAT), reduced glutathione (GSH), *N*-acetyl cysteine (NAC), mannitol (MAN) and superoxide dismutase (SOD) in the presence of ADR. Treatment of H9c2 cells with RA, CAT, GSH, NAC, MAN, or SOD, significantly reduced H9c2 cell death induced by ADR (Fig. 6A), and the effect of RA peaked at 20 μM when it was similar to 20 mM MAN. Moreover, RA (20 μg/mL) was found to have a greater protective effect than the known anti-oxidants probucol, alpha-tocopherol and ascorbic acid in this cell system (Fig. 6B). To investigate the effect of RA on intracellular ROS generation, cells were pretreated with 20 μg/mL RA for 30 min and then incubated with 2 μM ADR for 16 h or 500 μM H_2O_2 for 30 min. Intracellular ROS levels were then determined by flow cytometry using the peroxide-sensitive fluorescent probe DCF-DA (2′,7′-dichlorofluorescin diacetate), which in the presence of intracellular ROS is oxidized to fluorescent 2′,7′-dichlorofluorescein [18]. Flow cytometric analysis showed that intracellular ROS increased after treatment with 2 μM ADR for 16 h (Fig. 7A) and 500 μM H_2O_2 for 5 min (Fig. 7B). As was expected, RA pretreatment blocked intra-cellular ROS generation by ADR and H_2O_2 (Fig. 7A and B).

3.6. Mn-SOD may participate in the inhibition of ADR-induced apoptosis by RA

The SOD mimetic Mn-TBAP is a potent protective agent against cardiomyocyte injury caused by ADR. To determine whether Mn-TBAP inhibits the apoptotic effect of ADR on H9c2 cells, we examined the cytotoxic effect of ADR (2 μM) on H9c2 cells in the presence or absence of Mn-TBAP or $MnSO_4$ (a control) after 30 h by Trypan Blue assay. Mn-TBAP at 40 μM was found to significantly inhibit H9c2 cells from ADR-induced cardiotoxicity, but MnSO4 had no effect (Fig. 8A). To probe the inhibitory effect of RA on ADR-induced H9c2 cell death, we examined Mn-SOD and Cu/Zn-SOD expressional regulation by ADR. Fig. 8B shows that ADR treatment downregulated Mn-SOD and Cu/Zn-SOD protein in a time dependent manner, and that RA treatment recovered Mn-SOD and Cu/Zn-SOD expression in H9c2 cells (Fig. 8B).

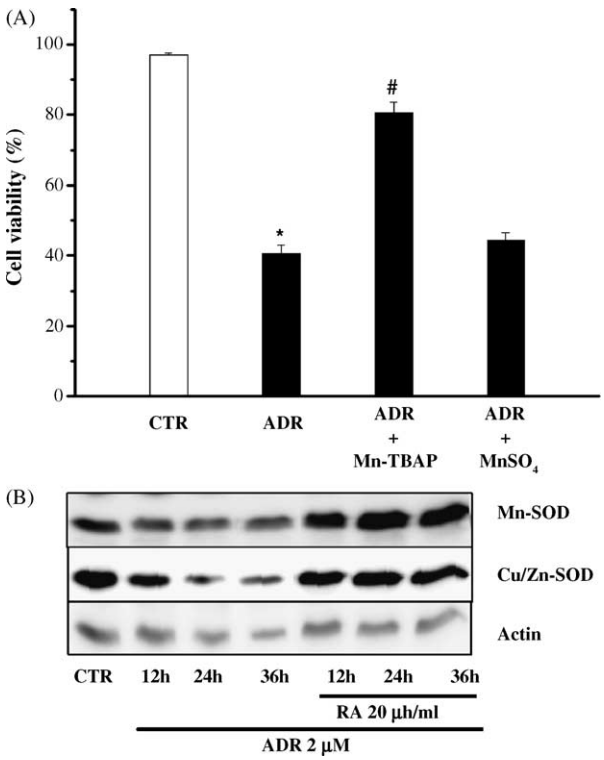

Fig. 8. The inhibitory effect of SOD on ADR-induced apoptosis in H9c2 cardiac muscle cells. (A) Cells were pretreated with/without 40 μM Mn-TBAP or 1 mM $MnSO_4$ for 30 min and then with 2 μM ADR. Trypan Blue assays were then performed. Data represent means ± S.E. ($n = 3$). $^{*}P < 0.05$; significantly different from control, $^{\#}P < 0.05$; significantly different from ADR only treated H9c2 cells. (B) Cells were pretreated with rosmarinic acid (20 μg/mL) for 30 min and then with ADR (2 μM) for the indicated times (10, 20, 30 h). Cell extracts immunoblotted using a anti-Mn-SOD, anti-Cu/Zn-SOD, and anti-α-actin antibodies, and immunoreactive bands were visualized using an LAS-3000.

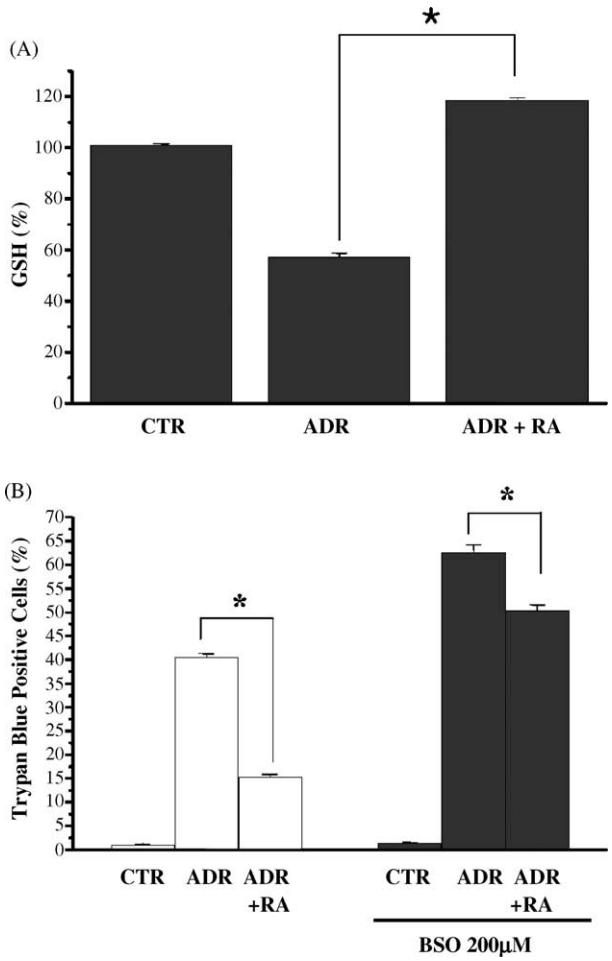

Fig. 9. The upregulation of GSH by RA. (A) Cells were pretreated with/without rosmarinic acid (20 μg/mL) for 30 h and then with 2 μM ADR, and cellular GSH levels were assessed. (B) Cells were pretreated with/without 200 μM BSO for 24 h, then with rosmarinic acid (20 μg/mL) for 30 min, and finally with 2 μM ADR for 30 h. Cell death was assessed by Trypan Blue assay. The data shown represent means ± S.E. ($n = 3$). $^{*}P < 0.01$; significantly different from ADR only treated H9c2 cells.

3.7. GSH is involved in the inhibition of ADR-induced apoptosis by RA

GSH is a potent intracellular anti-oxidant, and it has been reported that the depletion of GSH intracellularly enhances the susceptibility of cardiac toxicity and apoptosis [19]. Thus, we examined intracellular GSH expression in the presence or absence of ADR and/or RA. Fig. 8A shows that ADR treatment significantly reduced intracellular GSH levels, but that RA treatment increased GSH levels. BSO is a potent and selective inhibitor of glutamyl cysteinyl ligase, a rate-limiting enzyme in the synthesis of GSH. We pretreated cells with 200 μM BSO for 24 h, and after refreshing the medium, the cells were treated with 2 μM ADR in the absence or presence of 20 μg/mL RA. RA treatment was found to reduce ADR-induced cell death from 41 to 15%. However, in the presence of BSO, RA treatment reduced ADR-induced cell death from 15 to 50% (Fig. 9B). These, results suggest that RA-induced GSH upregulation is required for the inhibition of ADR by RA in H9c2 cardiac muscle cells.

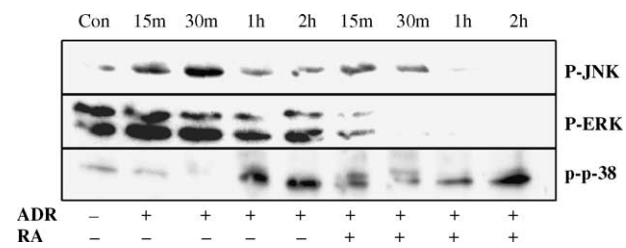

Fig. 10. The inhibitory effect of rosmarinic acid on the activation of MAPKs by ADR. Cells were pretreated with 20 μg/mL RA then treated with 2 μM. Cell extracts were immunoblotted using anti-phospho-JNK, anti-phospho-ERK, anti-phospho-p38, anti-JNK, anti-ERK, or anti-p38 antibodies.

3.8. RA inhibits JNK and ERK activation

We examined the activations of JNK, ERK and p38 in ADR-treated H9c2 cardiac muscle cells. The activation states of these components of the MAPK pathways were

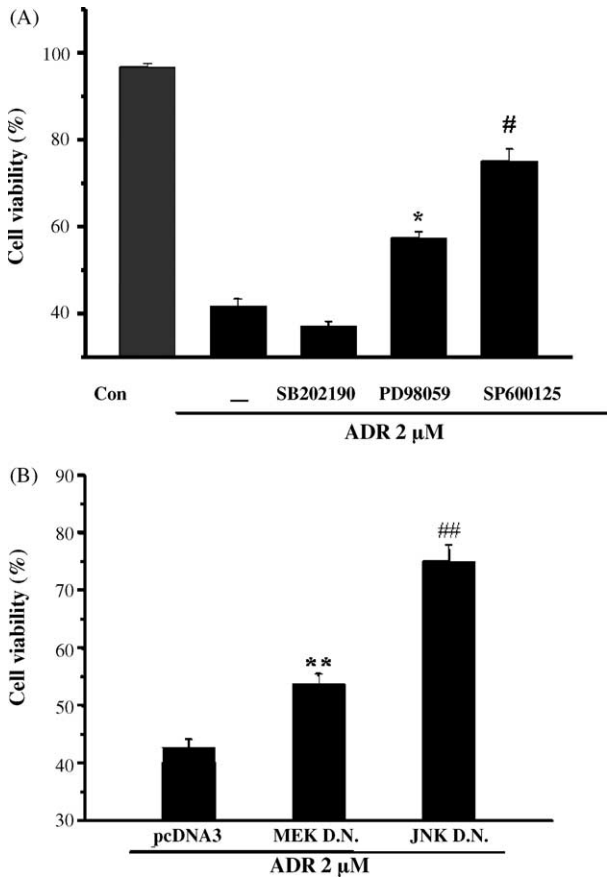

Fig. 11. The effects of JNK and ERK on H9c2 cell death induced by ADR. (A) Cells were co-treated with 2 μM ADR for 30 h in the presence or absence of the indicated inhibitors, i.e., SB202190 10 μM, PD98059 10 μM, or SP600125 10 μM. The data shown represent means ± S.E. ($n = 3$). $^{*}P < 0.05$ and $^{\#}P < 0.01$; significantly different from ADR only treated. (B) pcDNA3, JNK dominant negative, and ERK dominant negative cells were treated with 2 μM ADR for 30 h, and cell viability was determined by Trypan Blue assay. The data represent means ± S.E. ($n = 3$). $^{**}P < 0.05$, $^{\#\#}P < 0.01$; significantly different from pcDNA3-treated cells.

determined using commercially available antibodies that specifically recognize active (phosphorylated) forms. Cells were pretreated with 20 μg/mL RA for 30 min and then treated with 2 μM ADR for the indicated times (15 min, 30 min, 1 h, 2 h). RA was found to prevent the activation of JNK as well as ERK, but had no effect on the activations of p38 MAPK by ADR (Fig. 10). The total expressions of the three MAPKs were unchanged (data not shown). To deter-

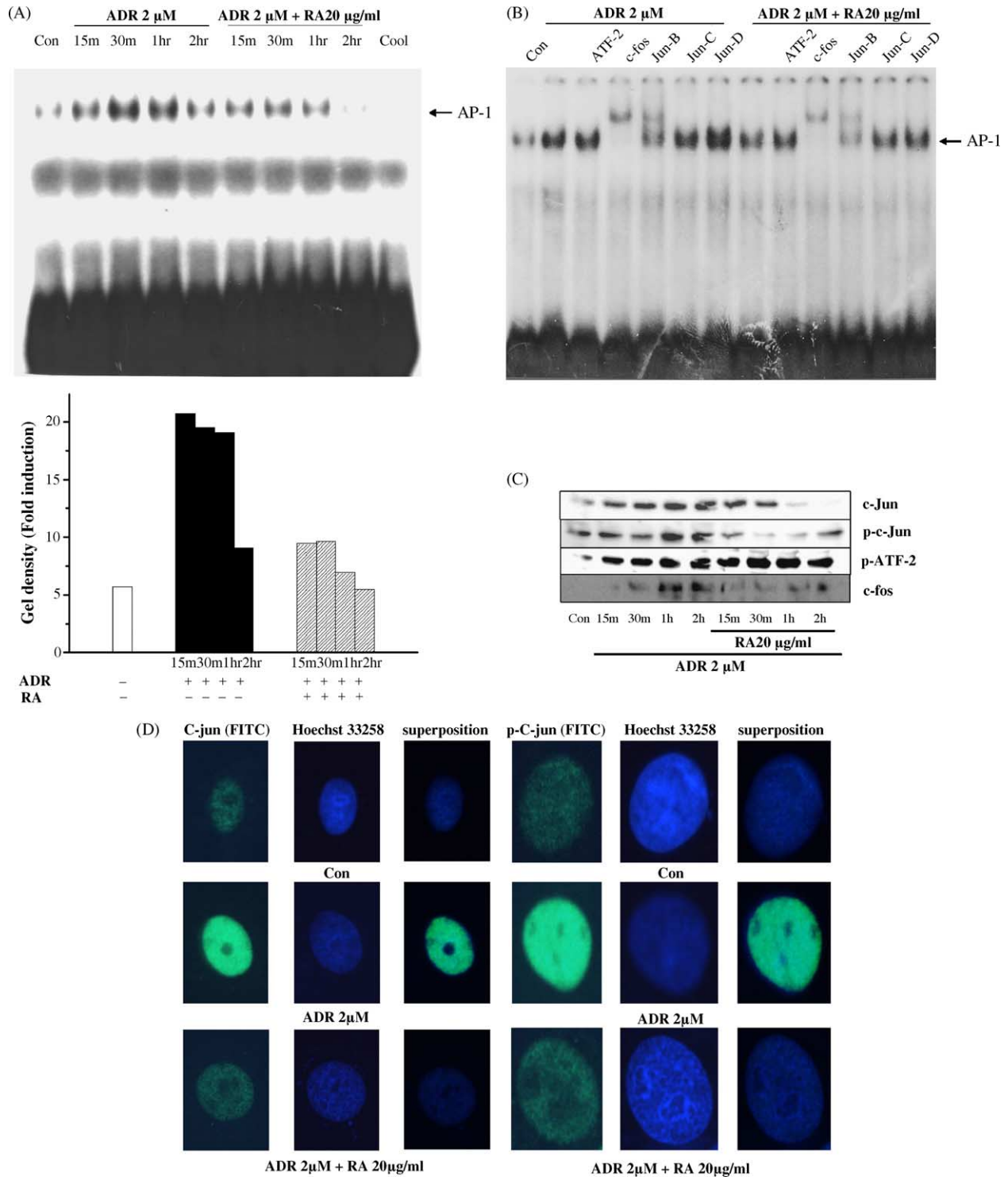

Fig. 12. Rosmarinic acid inhibition of AP-1 transcription factor activation by ADR. H9c2 cells were co-treated with 2 μM ADR for the indicated times in the absence or presence of 20 μg/mL RA. (A) Nuclear proteins were analyzed by electrophoretic mobility shift assay (EMSA) for binding to a γ-^{32}P labeled AP-1 consensus oligodeoxynucleotide. (B) Cells were co-treated with 2 μM ADR for 1 h in the absence or presence of 20 μg/mL RA. Nuclear extracts were subjected to EMSA in absence or presence of antibodies to the indicated AP-1. DNA binding activity was detected by autoradiography (A and B). (C) Cell extracts were examined by immunoblotting by probing with the indicated antibodies, and immunoreactive bands were visualized using an LAS-3000. (D) The cells were labeled with anti-c-Jun or anti-phospho-c-Jun antibodies, and nuclei were labeled with Hoechst 33258, and observed under a fluorescence microscope (original magnification 1000×).

mine whether the activations of these MAPKs are essential for ADR-induced apoptosis, we inhibited the activations of JNK and ERK, using the kinase inhibitors SP600125 and PD98059, respectively, or used the dominant negative cell lines JNK KD and MEK KD. All of these changes reduced ADR-induced apoptosis in H9c2 cells (Fig. 11A and B). These results indicate that JNK has an important role in ADR-induced apoptosis, and that ERK is also involved in this process, but to a lesser extent.

3.9. RA inhibits the activations of JNK and the transcription factor AP-1

H9c2 cells were pretreated with 20 μg/mL RA for 30 min and then treated with 2 μM ADR for the indicated times (15, 30, 60 and 120 min). Nuclear extracts were then prepared and incubated in the presence of a γ-^{32}P-labeled probe harboring the AP-1 consensus motif. Specificity was confirmed using cold (unlabeled) probe inhibitors. As shown in Fig. 12A, treatment of cells with ADR increased AP-1 activation, but RA pretreatment inhibited this activation.

AP-1 motifs (also known as TPA (12-*O*-tetradecanoylphorbol-13-acetate) response elements) commonly bind either Jun homodimers or Jun/Fos heterodimers. In particular, Jun family members are activated in a JNK-dependent manner by the phosphorylation of serine or threonine residues in their N-terminal regions [20,21], whereas Fos family members are activated by the ERK-dependent phosphorylation of Ser or Thr in their C-terminal region [22]. In order confirm that the protein bound to the probe was AP-1, a supershift experiment was performed using anti-ATF-2, anti-c-fos and anti-Jun family member (i.e., anti-c-Jun, anti-Jun-B, anti-Jun-D) antibodies. Our supershift assays indicated that ADR stimulated c-fos, Jun-B, c-Jun and p-c-Jun to bind to the distal AP-1 site, and that RA partially inhibits all of these effects of ADR (Fig. 12B). Moreover, RA inhibited the ADR-induced expressions of c-fos, Jun-B, c-Jun and p-c-Jun (Fig. 12C). In fact, c-Jun and p-c-Jun are widely regarded as an inevitable consequences of JNK activation. c-Jun and p-c-Jun subcellular localizations were studied following after exposing H9c2 cells to 2 μM ADR. Cells were grown on glass coverslips and pretreated or not with 20 μg/mL RA for 30 min and then treated with 2 μM ADR for 2 h. When cells were treated with ADR only activated c-Jun and p-c-Jun were observed in the nucleus, but RA prevented activated c-Jun and p-c-Jun nuclear accumulation (Fig. 12D). Our results suggest that RA inhibits ADR-induced AP-1 (c-fos, Jun-B, c-Jun and p-c-Jun) activation (Fig. 13).

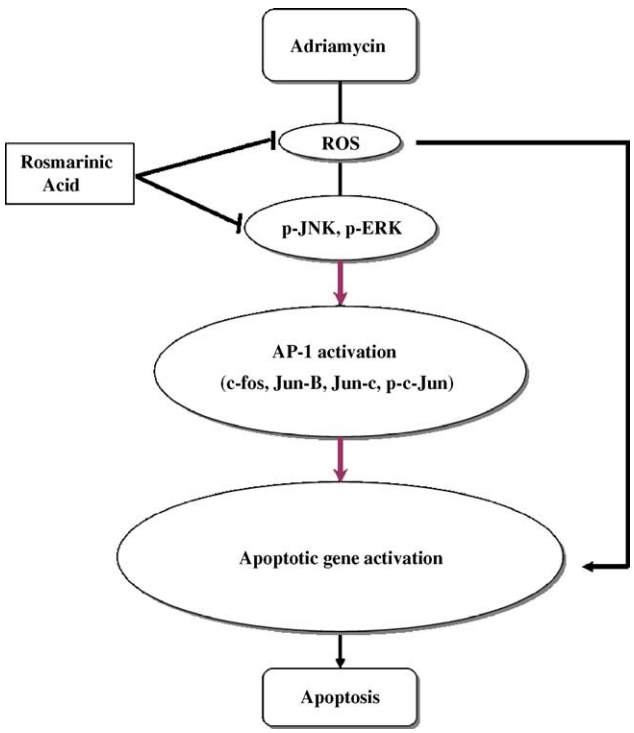

Fig. 13. Schematic of the inhibition of ADR-induced H9c2 cardiac muscle cell death by rosmarinic acid.

4. Discussion

This study shows that RA effectively protects cardiac muscle cells from ADR-induced cell death. Several studies have indicated that apoptosis occurs in the human heart during end stage cardiac failure or acute myocardial infarction, which suggests that apoptosis is involved in cardiovascular disease [23]. We expected at the beginning of this study that apoptosis is involved in the genesis of ADR-induced cardiomyopathy.

Bcl-2 is regarded as an important cellular component that guards against apoptotic cell death and which is also involved in many other cellular events. It has been reported that the prevention of apoptosis is associated with the upregulation of Bcl-2 and the downregulation of Bax [24,25]. Because the anti-apoptotic functions of Bcl-2 can be antagonized by pro-apoptotic proteins like Bax, the downregulation of Bax and the upregulation of Bcl-2 expression by RA might explain its anti-apoptotic effect (Fig. 3).

Moreover, ADR-induced ROS release, and RA attenuated this effect (Fig. 7). These observations highlight that RA has anti-oxidant properties in addition to its inhibition of ADR-induced cardiotoxicity.

ADR stimulates ROS release which may result in irreversible cardiomyopathy [8]. Most evidence supporting this relation was obtained from in vitro studies, and includes evidence that ADR increases lipid peroxidation and free radical production in heart tissue, and that free radical scavengers such as *N*-acetyl-cysteine, Vitamin E, superoxide dismutase and catalase reduce the severity of ADR-induced oxidative damage [26,27].

A number of studies have been undertaken to reduce ADR-induced cardiotoxicity. ICRF187 ((s)-(+)-1,2-bis

(3,5-dioxopiperazenyl) propane) has been approved Minotti and Schimmel as a treatment for those suffering from the cardiotoxic effects of anthracycline drugs. However, dexrazoxane (ICRF-187) is the only prophylactic treatment approved for use in cancer patients to prevent anthracycline-mediated cardiotoxicity. Its mode of action appears to be due to its ability to remove iron from iron/anthracycline complexes, and thus to reduce free radical formation by these complexes. Dexrazoxane also influences cell biology due to its ability to inhibit topoisomerase II and regulate cellular iron homeostasis. In a pilot study to assess the efficacy of ICRF187 [(s)-(+)-1,2-bis (3,5-dioxopiperazenyl) propane], it seemed to be provide highly effective cardioprotection to a small group of children with end-stage malignancy. Although the cardioprotective effect of dexrazoxane in cancer patients undergoing anthracycline-based therapy is well documented, the ability of this drug to modulate cellular iron metabolism and ROS release may led to its wider application in cancer therapy, immunology, or in the treatment of infectious disease. RA has a strong anti-apoptotic effect against ADR-induced cell death, which is similar to that of mannitol, and greater that those of NAC, SOD and catalase. In the present study, the anti-oxidant effect of RA was not compared with that of dexrazoxane. However, a comparative study of this type is warranted to determine whether RA can be used to prevent anthracycline-mediated cardiotoxicity in cancer patients.

In transgenic mice lines expressing elevated levels of Mn-SOD, electron microscopy revealed dose-dependent ultrastructural alterations and marked mitochondrial damage in non-transgenic mice treated with ADR [28]. They also showed that levels of serum creatine kinase and lactate dehydrogenase in ADR-treated mice were significantly higher than in non-transgenic mice than their transgenic littermates expressing high level of Mn-SOD after ADR treatment. These results support that free radical generation play a major role in ADR toxicity, and suggest that mitochondria are a critical site of cardiac injury. Consistent with these results, RA was found to stimulate Mn-SOD protein expression and a single treatment with ADR was found to reduce Mn-SOD protein expression in H9c2 cardiac muscle cells (Fig. 8B). These results show that the induction of Mn-SOD (using Mn-SOD mimetic agents-Mn-TBAP) inhibits ADR-induced cytotoxicity (Fig. 8A).

Intracellular GSH content was increased by RA (Fig. 9A). Furthermore, the depletion of glutathione by BSO, a γ-glutamyl cysteine synthetase inhibitor, in cardiac muscle cells increased their susceptibility to injury by ADR (Fig. 9B). BSO, a relatively specific inhibitor of glutathione biosynthesis, is frequently used to manipulate the level of glutathione in vitro and in vivo [29,30]. Substantial evidence suggests that multiple molecular mechanisms contribute to the cytoprotective action of GSH. GSH upregulation can promote non-enzymatic hydroxyl radical detoxification and inhibit ADR-induced cell death. Therefore, Mn-SOD and GSH upregulation by RA contribute to the scavenging of free radicals and thus inhibit cell death in cardiac muscle cells. This suggests that the RA-induced inhibition of apoptosis is associated with the regulations of Mn-SOD and GSH, and on its scavenging of free radicals in cardiac muscle cells.

Another characteristic feature of ADR is that it activates MAPK family members [31–33]. SP600125 or PD 98059 treated H9c2 cells, and dominant negative JNK and MEK1 mutant transfected H9c2 cells all showed ADR-induced cell inhibition (Fig. 11). Moreover, RA inhibited the ADR-induced activations JNK and ERK, suggesting that activated JNK and ERK are pro-apoptotic signals. The activation of ERK was previously found to suppress apoptotic induction by ADR [34,35], but paradoxically, ADR activates ERK and also induces apoptosis. The findings of the present study are consistent with two reports that suggested that ERK activation mediates apoptosis [36,37]. In addition, the functional significance of JNK activation in cell fate determination remains controversial. For example, JNK activated by NO or oxidative stress was found to inhibit apoptosis and thus promote cell survival [38,39], but on the other hand, JNK activation was found to play a pro-apoptotic role in the cell death of cardiac myocytes induced by ADR [40]. In addition, ADR that activated JNK, and also induced apoptosis, and ADR was also reported to activate AP-1 [41]. Previous studies have demonstrated that the AP-1 is an important regulator of proliferation, transformation, and apoptosis, depending on cell type [42,43]. Our results show that the inhibitions of JNK and ERK down-regulate the activation of AP-1 transcription factor, c-fos, Jun-B, c-Jun and p-c-Jun, which suggests that the inhibition of ADR-induced apoptosis by RA is associated with AP-1 inhibition.

In the present study, we found that CAT, GSH, NAC, MAN and SOD all significantly reduced ADR-induced H9c2 apoptosis, which suggest that ROS play an important role in the induction of ADR-induced apoptosis. Our data also show that RA has a greater anti-apoptotic effect than probucol, ascorbic acid and alpha-tocopherol. Although future studies are needed to examine whether RA has an anti-apoptotic effect in vivo, our results provide evidence for the first time that JNK and ERK activation can be pro-apoptotic in ADR-treated cardiac muscle cells, and strongly suggest that ROS is responsible for ADR-induced JNK, and ERK activation. In addition, these results also suggest that the inhibitory effect of RA is associated with the upregulation of Mn-SOD and GSH and its scavenging effect on free radicals in cardiac muscle cells.

Acknowledgments

This research was supported by the Korean Ministry of Science and Technology through the Korean Center for Healthcare Technology Development.

References

[1] Carter SK. ADR-a review. J Natl Cancer Inst 1975;55(6):1265–74.
[2] Hitchcock-Bryan S, Gelber R, Cassady JR, Sallan SE. The impact of induction anthracycline on long-term failure-free survival in childhood acute lymphoblastic leukaemia. Med Pediatr Oncol 1986;14(4):211–5.
[3] Zambetti M, Terenziani M, Bartoli C, Valagussa P, Piotti P, Ferranti C, et al. Intermediate doses of cyclophosphamide alone or following ADR in advanced breast cancer. A pilot study. Am J Clin Oncol 1996;19(1):82–6.
[4] Tack DK, Palmieri FM, Perez EA. Anthracycline vs nonanthracycline adjuvant therapy for breast cancer. Oncology (Huntingt) 2004;18(11): 1367–76.
[5] Singal PK, Iliskovic N. ADR-induced cardiomyopathy. N Engl J Med 1998;339(13):900–5.
[6] Fogli S, Nieri P, Breschi MC. The role of nitric oxide in anthracycline toxicity and prospects for pharmacologic prevention of cardiac damage. Federation Am Soc Exp Biol J 2004;18(April (6)):664–75.
[7] Kotamraju S, Konorev EA, Joseph J, Kalyanaraman B. ADR-induced apoptosis in endothelial cells and cardiomyocytes is ameliorated by nitrone spin traps and ebselen. Role of reactive oxygen and nitrogen species. J Biol Chem 2000;275:33585–92.
[8] Lee V, Randhawa AK, Singal PK. ADR-induced myocardial dysfunction in vitro is mediated by free radicals. Am J Physiol 1991;261(4 Pt 2):H989–95.
[9] Liu QY, Tan BK. Effects of cis-unsaturated fatty acids on ADR sensitivity in P388/DOX resistant and P388 parental cell lines. Life Sci 2000;67(10):1207–18.
[10] Zupko I, Hohmann J, Redei D, Falkay G, Janicsak G, Mathe I. Antioxidant activity of leaves of Salvia species in enzyme-dependent and enzyme-independent systems of lipid peroxidation and their phenolic constituents. Planta Med 2001;67(4):366–8.
[11] al-Sereiti MR, Abu-Amer KM, Sen P. Pharmacology of rosemary (Rosmarinus officinalis Linn.) and its therapeutic potentials. Indian J Exp Biol 1999;37(2):124–30.
[12] Ito H, Miyazaki T, Ono M, Sakurai H. Antiallergic activities of rabdosiin and its related compounds: chemical and biochemical evaluations. Bioorg Med Chem 1998;6(7):1051–6.
[13] Chlopcikova S, Psotova J, Miketova P, Sousek J, Lichnovsky V, Simanek V. Chemoprotective effect of plant phenolics against anthracycline-induced toxicity on rat cardiomyocytes. Part II. caffeic, chlorogenic and rosmarinic acids. Phytother Res 2004;18(5):408–13.
[14] Woo ER, Piao MS. Antioxidative constituents from Lycopus lucidus. Arch Pharm Res 2004;27(2):173–6.
[15] Winters RA, Zukowski J, Ercal N, Matthews RH, Spitz DR. Analysis of glutathione, glutathione disulfide, cysteine, homocysteine, and other biological thiols by high-performance liquid chromatography following derivatization by *n*-(1-pyrenyl)maleimide. Anal Biochem 1995;227(1):14–21.
[16] Sutton VR, Vaux DL, Trapani JA. Bcl-2 prevents apoptosis induced by perforin and granzyme B, but not that mediated by whole cytotoxic lymphocytes. J Immunol 1997;158(12):5783–90.
[17] Budihardjo I, Oliver H, Lutter M, Luo X, Wang X. Biochemical pathways of caspase activation during apoptosis. Annu Rev Cell Dev Biol 1999;15:269–90.
[18] Zweier JL. Measurement of superoxide-derived free radicals in the reperfused heart. Evidence for a free radical mechanism of reperfusion injury. J Biol Chem 1998;263(3):1353–7.
[19] Jiang N, Dreher KL, Dye JA, Li Y, Richards JH, Martin LD, et al. Residual oil fly ash induces cytotoxicity and mucin secretion by guinea pig tracheal epithelial cells via an oxidant-mediated mechanism. Toxicol Appl Pharmacol 2000;163(3):221–30.
[20] Pulverer BJ, Kyriakis JM, Avruch J, Nikolakaki E, Woodgett JR. Phosphorylation of c-jun mediated by MAP kinases. Nature 1991; 353(6345):670–4.
[21] Smeal T, Binetruy B, Mercola DA, Birrer M, Karin M. Oncogenic and transcriptional cooperation with Ha-Ras requires phosphorylation of c-Jun on serines 63 and 73. Nature 1991;354(6353):494–6.
[22] Murakami M, Ui M, Iba H. Fra-2-positive autoregulatory loop triggered by mitogen-activated protein kinase (MAPK) and Fra-2 phosphorylation sites by MAPK. Cell Growth Differ 1999;10(5): 333–42.
[23] Formigli L, Ibba-Manneschi L, Perna AM, Nediani C, Liguori P, Tani A, et al. Ischemia–reperfusion-induced apoptosis and p53 expression in the course of rat heterotopic heart transplantation. Microvasc Res 1998;56(3):277–81.
[24] Shihab FS, Andoh TF, Tanner AM, Yi H, Bennett WM. Expression of apoptosis regulatory genes in chronic cyclosporine nephrotoxicity favors apoptosis. Kidney Int 1999;56(6):2147–59.
[25] Wang S, Wang Z, Boise L, Dent P, Grant S. Loss of the bcl-2 phosphorylation loop domain increases resistance of human leukemia cells (U937) to paclitaxel-mediated mitochondrial dysfunction and apoptosis. Biochem Biophys Res Commun 1999;259(1):67–72.
[26] Geetha A, Sankar R, Devi CS. Effect of alpha-tocopherol on peroxidative membrane damage caused by ADR: an in vitro study in human erythrocytes. Indian J Exp Biol 1989;27(3):274–8.
[27] Kang YJ, Chen Y, Epstein PN. Suppression of ADR cardiotoxicity by overexpression of catalase in the heart of transgenic mice. J Biol Chem 1996;271(21):12610–6.
[28] Yen HC, Oberley TD, Gairola CG, Szweda LI, St. Clair DK. Manganese superoxide dismutase protects mitochondrial complex I against adriamycin-induced cardiomyopathy in transgenic mice. Arch Biochem Biophys 1999;362(1):59–66.
[29] Kim KS, Moon WS, Song HW, Kim JH, Cho SN. A case of persistent endometriosis after total hysterectomy with both salpingo-oophorectomy managed by radiation therapy. Arch Gynecol Obstet 2001; 265(4):225–7.
[30] Mohamed HE, El-Swefy SE, Hagar HH. The protective effect of glutathione administration on ADR-induced acute cardiac toxicity in rats. Pharmacol Res 2000;42(2):115–21.
[31] Kang YJ, Zhou ZX, Wang GW, Buridi A, Klein JB. Suppression by metallothionein of ADR-induced cardiomyocyte apoptosis through inhibition of p38 mitogen-activated protein kinases. J Biol Chem 2000;275(18):13690–8.
[32] Osborn MT, Chambers TC. Role of the stress-activated/c-Jun NH2-terminal protein kinase pathway in the cellular response to ADR and other chemotherapeutic drugs. J Biol Chem 1996;271(48): 30950–5.
[33] Yu R, Shtil AA, Tan TH, Roninson IB, Kong AN. ADR activates c-jun N-terminal kinase in human leukemia cells: a relevance to apoptosis. Cancer Lett 1996;107(1):73–81.
[34] Zhu W, Zou Y, Aikawa R, Harada K, Kudoh S, Uozumi H, et al. MAPK superfamily plays an important role in daunomycin-induced apoptosis of cardiac myocytes. Circulation 1999;100(20): 2100–7.
[35] Yue TL, Wang C, Gu JL, Ma XL, Kumar S, Lee JC, et al. Inhibition of extracellular signal-regulated kinase enhances ischemia/reoxygenation-induced apoptosis in cultured cardiac myocytes and exaggerates reperfusion injury in isolated perfused heart. Circ Res 2000; 86(6):692–9.
[36] Tang D, Wu D, Hirao A, Lahti JM, Liu L, Mazza B, et al. ERK activation mediates cell cycle arrest and apoptosis after DNA damage independently of p53. J Biol Chem 2002;277(15):12710–7.
[37] Woessmann W, Chen X, Borkhardt A. Ras-mediated activation of ERK by cisplatin induces cell death independently of p53 in osteosarcoma and neuroblastoma cell lines. Cancer Chemother Pharmacol 2002;50(5):397–404.
[38] Minamino T, Yujiri T, Papst PJ, Chan ED, Johnson GL, Terada N. MEKK1 suppresses oxidative stress-induced apoptosis of embryonic stem cell-derived cardiac myocytes. Proc Natl Acad Sci USA 1999;96(26):15127–32.

[39] Andreka P, Zang J, Dougherty C, Slepak TI, Webster KA, Bishopric NH. Cytoprotection by Jun kinase during nitric oxide-induced cardiac myocyte apoptosis. Circ Res 2001;88(3):305–12.
[40] Nobori K, Ito H, Tamamori-Adachi M, Adachi S, Ono Y, Kawauchi J, et al. ATF3 inhibits ADR-induced apoptosis in cardiac myocytes: a novel cardioprotective role of ATF3. J Mol Cell Cardiol 2002;34(10):1387–97.
[41] Liu Y, Ludes-Meyers J, Zhang Y, Munoz-Medellin D, Kim HT, Lu C, et al. Inhibition of AP-1 transcription factor causes blockade of multiple signal transduction pathways and inhibits breast cancer growth. Oncogene 2002;21(50):7680–9.
[42] Brown PH, Alani R, Preis LH, Szabo E, Birrer MJ. Suppression of oncogene-induced transformation by a deletion mutant of c-jun. Oncogene 1993;8(4):877–86.
[43] Liebermann DA, Gregory B, Hoffman B. AP-1 (Fos/Jun) transcription factors in hematopoietic differentiation and apoptosis. Int J Oncol 1998;12(3):685–700.